

# Numerical methods for reduced Vlasov equation

P. Helluy, L. Navoret, N. Pham

Inria Tonus & IRMA University of Strasbourg

NUMKIN 2016, IRMA, Octobre 20th 2016

# Plan

- 1 Model reduction
- 2 Numerical methods and objectives
- 3 Numerical results
- 4 Perspectives

# Model reduction of the Vlasov-Poisson equation

Vlasov equation :

$$\frac{\partial f}{\partial t}(\mathbf{x}, \mathbf{v}, t) + \mathbf{v} \cdot \nabla_{\mathbf{x}} f(\mathbf{x}, \mathbf{v}, t) + \mathbf{E} \cdot \nabla_{\mathbf{v}} f(\mathbf{x}, \mathbf{v}, t) = 0. \quad (1)$$

- $f(\mathbf{x}, \mathbf{v}, t)$  : distribution function at time  $t \geq 0$ , with position  $\mathbf{x} = (x_1, x_2, x_3) \in \Omega_{\mathbf{x}} \subset \mathbb{R}^3$  and velocity  $\mathbf{v} \in \Omega_{\mathbf{v}} \subset \mathbb{R}^3$
- $\mathbf{E}(\mathbf{x}, t)$  : electric field which satisfies the Poisson equation

$$\mathbf{E} = -\nabla_{\mathbf{x}} \Phi, \quad \text{with} \quad -\Delta_{\mathbf{x}} \Phi = \rho - 1. \quad (2)$$

- the charge density

$$\rho(\mathbf{x}, t) = \int_{\Omega_{\mathbf{v}}} f(\mathbf{x}, \mathbf{v}, t) d\mathbf{v}, \quad (3)$$

# Boundary condition

In practice  $\Omega_{\mathbf{x}} = ]0, L[^3$ , with  $L > 0$  and  $\Omega_{\mathbf{v}} = ] - V_{\max}, V_{\max}[^3$ , where  $V_{\max} > 0$  is the maximal velocity

## Boundary condition

- Periodical boundary condition in space :
- Outflow boundary condition in velocity :

$$(\mathbf{E}(\mathbf{x}, t) \cdot n_{\mathbf{v}})^- f(\mathbf{x}, \mathbf{v}, t) = 0$$

where  $n_{\mathbf{v}}$  be the outward normal unit vector on  $\partial\Omega_{\mathbf{v}}$

# Reduced Vlasov equation

Weak formulation : Find  $f \in V = \{f \in L^2(\Omega_{\mathbf{v}}), \mathbf{E} \cdot \nabla_{\mathbf{v}} f \in L^2(\Omega_{\mathbf{v}})\}$

$$\partial_t \int_{\Omega_{\mathbf{v}}} f \varphi + \nabla_{\mathbf{x}} \cdot \int_{\Omega_{\mathbf{v}}} \mathbf{v} f \varphi + \mathbf{E} \cdot \int_{\Omega_{\mathbf{v}}} \nabla_{\mathbf{v}} f \varphi - \beta \int_{\partial\Omega_{\mathbf{v}}} (\mathbf{E} \cdot \mathbf{n}_{\mathbf{v}})^- f \varphi = 0, \quad (4)$$

with any test function  $\varphi \in V$  and where  $\beta$  is a positive constant.

The distribution function is approximated by

$$f(\mathbf{x}, \mathbf{v}, t) \approx \sum_{j=1}^{N_{\mathbf{v}}} w_j(\mathbf{x}, t) \varphi_j(\mathbf{v}). \quad (5)$$

We obtain the reduced Vlasov equation

$$\mathcal{M} \partial_t \mathbf{w} + A^k \partial_{x_k} \mathbf{w} + B(\mathbf{E}) \mathbf{w} = 0, \quad k = 1 \dots 3. \quad (6)$$

# Reduced Vlasov equation

## Reduced Vlasov equation

$$\mathcal{M}\partial_t \mathbf{w} + A^k \partial_{x_k} \mathbf{w} + B(\mathbf{E})\mathbf{w} = 0, \quad k = 1 \dots 3.$$

In which  $\mathbf{w} = (w_1, w_2, \dots, w_{N_v})^T$ . The mass matrix  $\mathcal{M}$ ,  $A^k$ ,  $k = 1 \dots 3$  and  $B(\mathbf{E})$  are matrices of dimension  $N_v \times N_v$ , whose elements are given by

$$\mathcal{M}_{ij} = \int_{\Omega_v} \varphi_i \varphi_j, \quad A_{ij}^k = \int_{\Omega_v} v_k \varphi_i \varphi_j, \quad k = 1 \dots 3, \quad (7)$$

$$B(\mathbf{E})_{ij} = \int_{\Omega_v} \varphi_i (\mathbf{E} \cdot \nabla_v) \varphi_j - \beta \int_{\partial\Omega_v} (\mathbf{E} \cdot \mathbf{n}_v)^- \varphi_j \varphi_i. \quad (8)$$

# Reduced Vlasov equation

## Properties

- The system depends only on  $\mathbf{x}$  variable and not on the  $(\mathbf{x}, \mathbf{v})$  variables
- $\mathcal{M}$  is symmetric positive-definite,  $A^k$  is symmetric,  $k = 1, 2, 3$ ,  $B(\mathbf{E})$  is “almost” skew-symmetric (except on boundaries)
- Hyperbolic system
- For  $1/2 \leq \beta \leq 1$ , the reduced Vlasov equation is  $L^2$  stable

$$\frac{1}{2} \frac{d}{dt} \left( \int_{\Omega_{\mathbf{x}} \times \Omega_{\mathbf{v}}} f^2 \right) \leq -\frac{1}{2} \int_{\Omega_{\mathbf{x}} \times \partial\Omega_{\mathbf{v}}} (\mathbf{E} \cdot \mathbf{n}_{\mathbf{v}})^+ f^2, \quad (9)$$

- Loss of total charge

$$\frac{d}{dt} \rho_{\text{tot}} = - \int_{\Omega_{\mathbf{x}} \times \partial\Omega_{\mathbf{v}}} (\mathbf{E} \cdot \mathbf{n}_{\mathbf{v}})^+ f, \quad (10)$$

# Plan

- 1 Model reduction
- 2 Numerical methods and objectives**
- 3 Numerical results
- 4 Perspectives



# Numerical methods and objectives

Resolution of the hyperbolic system :

- Finite volume (SeLaLib)
- Semi-Lagrangian (SeLaLib)
- Discontinuous Galerkin (CLAC, SCHNAPS)

Objectives :

- Implementation of the three methods
- Comparison between the three methods

# Finite volume scheme (2D)

Reduced Vlasov equation in 2D

$$\partial_t \mathbf{w} + \mathcal{M}^{-1} A^1 \partial_{x_1} \mathbf{w} + \mathcal{M}^{-1} A^2 \partial_{x_2} \mathbf{w} + \mathcal{M}^{-1} B(E) \mathbf{w} = 0$$

- Finite-volume approximation

$$\begin{aligned} \partial_t \mathbf{w}_{kl} = & - \frac{\mathcal{F}(\mathbf{w}_{k,l}, \mathbf{w}_{k+1,l}, \nu^1) - \mathcal{F}(\mathbf{w}_{k-1,l}, \mathbf{w}_{k,l}, \nu^1)}{h_1} \\ & - \frac{\mathcal{F}(\mathbf{w}_{k,l}, \mathbf{w}_{k,l+1}, \nu^2) - \mathcal{F}(\mathbf{w}_{k,l-1}, \mathbf{w}_{k,l}, \nu^2)}{h_2} + S(\mathbf{w}_{kl}) \end{aligned}$$

$$\nu^1 = (1, 0) \text{ and } \nu^2 = (0, 1)$$

- Viscous flux

$$\mathcal{F}(\mathbf{w}_L, \mathbf{w}_R, \nu) = \mathcal{M}^{-1} A_i \nu_i \frac{\mathbf{w}_L + \mathbf{w}_R}{2} - \kappa \frac{(\mathbf{w}_R - \mathbf{w}_L)}{2}, \quad \text{with } \kappa \geq 0. \quad (11)$$

where  $\kappa$  : numerical diffusion.

# Finite volume scheme (2D) - Stability

Time discretization : Runge-Kutta (RK) of order 1, 2, 3 ou 4.

- ① For the centered flux
  - RK1 and RK2 schemes are unstable
  - RK3 and RK4 schemes : there exists a constant  $\varphi \in (0, 1)$  such that the schemes are stable under the CFL condition  $\Delta t = \varphi \frac{\Delta x}{V_{\max}}$ .
- ② For the viscous flux : The Runge-Kutta schemes of order 1, 2, 3, 4 with the **viscous** flux are all stable when taking  $\Delta t$  sufficiently small (CFL condition).
  - RK1 and RK2 : CFL parameter depends on  $\kappa$
  - RK3 and RK4 schemes : CFL parameter does not depend on  $\kappa$

# Finite volume scheme (2D) - Implementation

## Implementation

- SeLaLib library
- MPI parallelization

## Drawbacks

- Matrix inversion (skyline storage of band matrices)
- stability under CFL condition (in space and velocity)
- low spatial accuracy

## Advantages

- locally conservative (mass, momentum) and  $L^2$  stable
- finite-element refinement in the velocity direction
- numerical dissipation only on the spatial direction

# Semi-Lagrangian scheme (2D)

Lagrange polynomials and Gauss-Lobatto points  $\Rightarrow$  diagonal matrices

$$M^{-1}A^i = \begin{pmatrix} v_1^i & & \\ & \ddots & \\ & & v_{N_v}^i \end{pmatrix} \Rightarrow \text{Semi-Lagrangian approximation}$$

Splitting method

- Advection in the  $x_1$  direction (1D Semi-Lagrangian)
- Advection in the  $x_2$  direction (1D Semi-Lagrangian)
- Addition of the source term

Advantages :

- No CFL condition (in space)
- High order method

Implementation :

- Selalib library
- MPI parallelization

Drawbacks :

- Mass conservative on uniform 1D mesh
- difficult to extend to non-cartesian mesh

# Discontinuous Galerkin scheme - Drift-kinetic model

In a cylinder consider a strong homogeneous magnetic field  $\mathbf{B}_{\text{app}} = b \mathbf{e}_3$ ,  
the Vlasov equation

$$\frac{\partial f}{\partial t} + \mathbf{v} \cdot \nabla_{\mathbf{x}} f + (\mathbf{E} + \mathbf{v} \times \mathbf{B}_{\text{app}}) \cdot \nabla_{\mathbf{v}} f = 0.$$

becomes the drift-kinetic equation

$$\partial_t f + \mathbf{E}_{\perp} \cdot \nabla_{\mathbf{x}_{\perp}} f + v_{\parallel} \partial_{x_{\parallel}} f + E_{\parallel} \partial_{v_{\parallel}} f = 0. \quad (12)$$

Weak formulation (in velocity) of drift-kinetic equation

$$\mathcal{M} \partial_t \mathbf{w} + \mathbf{E}_{\perp} \cdot \mathcal{M} \nabla_{\perp} \mathbf{w} + A \partial_{x_{\parallel}} \mathbf{w} + B(E_{x_{\parallel}}) \mathbf{w} = 0. \quad (13)$$

# Discontinuous Galerkin scheme - Drift-kinetic model

Weak upwind DG formulation

$$\begin{aligned}
 & \int_L \partial_t \mathbf{w}^L \cdot \psi_L - \int_L E_{\perp} \mathbf{w}^L \cdot \nabla_{\perp} \psi^L + \int_{\partial L \cap \Omega_{\mathbf{x}}} E_{\perp} (n^+ \mathbf{w}_L + n^- \mathbf{w}_R) \cdot \psi_L + \\
 & \int_L \mathbf{w}^L \cdot (\mathcal{M}^{-1} A) \partial_3 \psi^L + \int_{\partial L \cap \Omega_{\mathbf{x}}} ((\mathcal{M}^{-1} A) n_3^+ \mathbf{w}_L + (\mathcal{M}^{-1} A) n_3^- \mathbf{w}_R) \cdot \psi_L + \\
 & \int_L (\mathcal{M}^{-1} B(E_{X_3})) \mathbf{w}^L \cdot \psi^L = 0
 \end{aligned} \tag{14}$$

where  $n$  the normal vector on  $\partial L$  oriented from the cell  $L$  to the neighboring cells  $R$ ,  $\psi_{L,k}$  : test function.

# Discontinuous Galerkin scheme

## Implementation :

- SCHNAPS code
- multipatch, curved hexahedron mesh (gmsh)
- GPU parallelization (OpenCL)
- Starpu (task distribution)

## Drawbacks :

- CFL condition (in velocity and space)

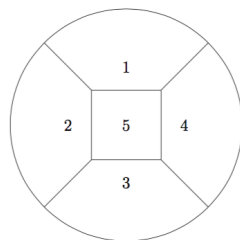


FIGURE: Macro-mesh of a simple disk

## Advantages :

- high-order accuracy
- handle complex geometry
- parallelization



# Plan

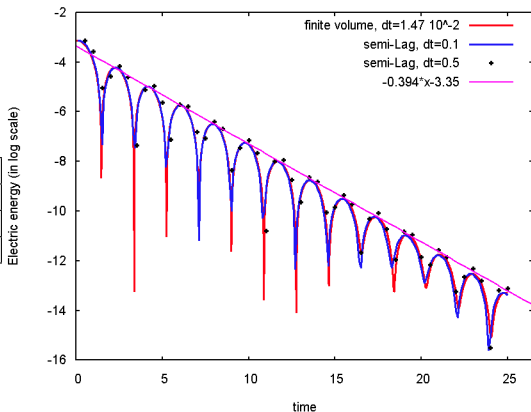
- 1 Model reduction
- 2 Numerical methods and objectives
- 3 Numerical results**
- 4 Perspectives

## 2D Landau damping

Initial distribution function :  $f_0(x, v) = \frac{1}{2\pi}(1 + \varepsilon \cos(k_1 x_1) \cos(k_2 x_2))e^{-\frac{(v_1^2 + v_2^2)}{2}}$ .

Parameters :  $k_1 = k_2 = 0.5$ ,  $\varepsilon = 5 \times 10^{-3}$ ;  $x \in [0, 4\pi] \times [0, 4\pi]$ ,  $v \in ]-6, 6[ \times ]-6, 6[$ ;  
 $N_1 = N_2 = 32$  (space),  $NC_1 = NC_2 = 32$ , degree 2 (velocity); 4 processors.

	$\Delta t$	cpu time (s)
FV	$1.47 \cdot 10^{-2}$	10182
SL	0.1	748
SL	0.5	171



# Speed-up

2D Landau damping : Computed on the supercomputer Curie (TGCC).  
 Parameters : 100 iterations,  $256^2 \times 65^2 \approx 277.10^6$  unknowns

Number of CPU	4	8	16	32	64	128
computation time	21280	13992	7237	3685	1869	985
speed-up (relative)		1.52	1.93	1.96	1.97	1.89
speed-up		6.08	11.76	23.1	45.53	86.41

**TABLE:** Computational time and speedup for the 2D **finite-volume** code.

Number of processor units (CPU)	8	16	64	128
computation time (second)	7398	3673	943	491
speed-up (relative)		2.01	3.89	1.92
speed-up		16.11	62.76	120.54

**TABLE:** Computational time and speedup for the 2D **semi-Lagrangian** code.

# Efficiency of code

The efficiency defined by

$$\text{eff} := \frac{s * nb_{points} * nb_{iterations}}{T * 10^6 * nb_{processors}}. \quad (15)$$

- With the finite volume code,  $\text{eff} = 1.75$
- With the semi-Lagrangian code,  $\text{eff} = 3.5$ .

→ The efficiency of semi-Lagrangian method is twice as much than this of the finite volumes method. Reason : semi-Lagrangian is without matrices inversions.

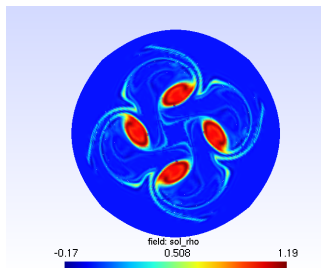
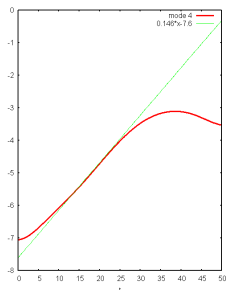
# Guiding center model

- Guiding center model in a disc

$$\partial_t \rho + \mathbf{E}^\perp \cdot \nabla_x \rho = 0$$

$$-\Delta_x \Phi = \rho - \bar{\rho}, \quad \mathbf{E} = -\nabla_x \Phi$$

- Diocotron instability test-case [Davidson, 2013] : perturbed annular electron layer



Growth-rate of the 4th Fourier mode

$\rho$  at time  $t = 100$

# Speed-up

Computational time and speedup for the 2D schnaps code on CPU.  
 Computed on the Irma Atlas cluster. Parameters : 20 iterations,  $M_x = 20$   
 $d_x = 3$ ,  $N_v = 31$ ,  $d_v = 3$ ,  $M_v = 20$ .

	sequential code 1 core	OpenCL code 1 core	OpenCL code 1GPU
20 iterations	3532	2401.3	39.2
1 iterations	168.19	114.34	1.8
relative speed-up		1.47	63.5

Nb of CPU	1	2	4	8	16	32	64
comp. time	2401.3	1396.12	801.39	504.6	276.89	193.9	142.5
speed-up		1.72	2.997	4.759	8.67	12.38	16.9

# Plan

- 1 Model reduction
- 2 Numerical methods and objectives
- 3 Numerical results
- 4 Perspectives**

# Perspectives

- 1 Apply the code in `schnaps` to solve the drift-kinetic model and the gyro-kinetic model.
- 2 Resolve the drift-kinetic in `SELALIB` to compare with the one in `schnaps`.
- 3 Study the Vlasov model with the collision term.



THANKS FOR YOUR  
ATTENTION!